

1 *This paper is a non-peer reviewed preprint submitted to EarthArXiv. The manuscript is submitted to Soil*
2 *Biology and Biochemistry and currently under peer review. Future updates on this manuscript will be*
3 *provided once it's peer-reviewed or accepted. Please feel free to contact me at:*
4 arjun.chakrawal@pnnl.gov *if you have any questions or feedbacks.*

5

6 **Challenges in Integrating DOM Chemodiversity into Kinetic Models of Soil Respiration for Improved**
7 **Carbon Cycling Predictions**

8 Arjun Chakrawal¹, Odeta Qafoku¹, Satish Karra¹, John Bargar¹, and Emily Graham^{1,2}

9 ¹Environmental Molecular Sciences Laboratory (EMSL), Pacific Northwest National Laboratory, PO Box
10 999, Richland, WA 99352, USA

11 ²School of Biological Sciences, Washington State University, Pullman, WA, USA

12 **1. Abstract:**

13 Chemodiversity of dissolved organic matter (DOM) has been proposed as an ecosystem property
14 controlling the microbial metabolism; thus, the fate of carbon (C) in soils. Recent research suggests that
15 accounting for DOM chemodiversity can improve the accuracy of process-based C cycling models;
16 however, this approach has never been validated at continental U.S. scale. In this study, we used
17 statistical and kinetic modeling approaches to evaluate how DOM chemodiversity affects soil respiration
18 and whether incorporating it in kinetic models improves respiration prediction. We utilized paired high
19 resolution FTICR-MS descriptions of DOM chemistry and soil respiration rate measurements from 63
20 topsoils across the USA, provided by the Molecular Observation Network. Regression analysis revealed
21 that DOM alpha diversity (defined as the number of detected organic compounds) interacted nonlinearly
22 with dissolved organic C (DOC) and water-extractable total nitrogen (WETN) concentrations. Soils with
23 high DOC and WETN concentrations, showed decreased soil respiration with increasing alpha diversity,
24 while soils with low DOC and WETN concentrations showed increased respiration. Therefore, DOM
25 chemodiversity controlled the plausible tradeoff in microbial metabolism leading to either loss of C
26 through respiration or SOM buildup through increased microbial growth. This finding implies that
27 chemodiversity, as a parameter, has the potential to increase the accuracy of soil C cycling models. To
28 evaluate respiration rate dependence on chemodiversity as a parameter, we tested three kinetic models:
29 (1) as a function of DOC concentration only, (2) with model parameters informed by average DOM
30 chemodiversity and (3) by chemodiversity calculated within chemical classes of DOM. All three models
31 predicted respiration with similar accuracy. This inability suggests that current kinetic formulations do
32 not adequately represent chemodiversity–microbial metabolism interactions. Therefore, we advise
33 future studies to explore the effects of DOM chemodiversity, with consideration of its interactions with
34 tradeoffs in microbial traits and environmental conditions.

35 **Keywords:** FTICR-MS, bioenergetic, soil organic matter, soil respiration, chemodiversity, carbon cycle
36 modeling

37 **2. Introduction**

38 Dissolved organic matter (DOM) plays a significant role in terrestrial systems, fueling microbial
39 metabolism, has been a key source of uncertainty in Earth Systems Models. Accurate characterization
40 and representation of DOM in Earth System Models is essential for quantifying carbon fluxes and
41 assessing the impacts of climate and environmental disturbances on soils (Tanentzap and Fonvielle,
42 2024). Most soil C cycling models aiming to predict greenhouse gas fluxes simplify SOM pools into a few
43 chemically and/or physically distinct pools, and then may further constrain DOM dynamics using steady-

44 state assumption due to its putative high bioavailability. Indeed, the DOM pool has faster turnover time
45 compared to more refractory C fractions in soil (Wutzler et al., 2017), and its chemodiversity may directly
46 relate to the balance of soil organic matter decomposition vs. persistence (Ding et al., 2020; Kothawala
47 et al., 2021). Yet, effectively integrating DOM chemistry in soil C cycle models to improve predictions of C
48 stocks and fluxes beyond DOM pool size remains unresolved (Graham and Hofmockel, 2022).

49 Traditional soil carbon cycle models incorporate the chemical complexity of soil organic matter through
50 discrete pools representing varying degrees of SOM physicochemical recalcitrance, characterized using
51 linear kinetic parameters (Parton et al., 1994). More recent models have improved upon this abstraction
52 by conceptually dividing SOM into plant-derived, mineral-associated, dissolved, and microbial carbon
53 pools (Abramoff et al., 2018; Robertson et al., 2019; Wang et al., 2013; Wieder et al., 2014). Despite
54 numerous studies highlighting the chemodiversity of organic compounds found in particulate organic
55 matter (Witzgall et al., 2021), mineral-associated organic matter (Anderson et al., 2023; Lv et al., 2020)
56 and DOM (Ayala-Ortiz et al., 2023; Bahureksa et al., 2021), most models still consider these pools to be
57 chemically homogeneous and define their decomposition rates using fixed kinetic parameters. The fixed
58 parameters approach may be problematic for DOM pool metabolism because the choice of a parameter
59 may not represent the chemodiversity found in DOM. Furthermore, models based on Monod kinetics
60 typically use bulk chemistry (i.e., DOC concentration) to define the rate of microbial utilization (Camino-
61 Serrano et al., 2018; Yu et al., 2020). Such simplification overlooks the microbially induced
62 transformations of organic matter, and the intricate interactions between microbial uptake, release
63 (Amenabar et al., 2017; Marschmann et al., 2024), and sorption of DOM on mineral reactive surfaces
64 (Keiluweit et al., 2015; Sokol et al., 2019), all of which ultimately dictate chemical diversity and microbial
65 metabolism of DOM.

66 New measurement capabilities have also advanced our empirical understanding of DOM—high resolution
67 mass spectrometry methods can now detect tens of thousands of organic compounds—coincident with
68 emerging modeling approaches to account for this extraordinary chemical and thermodynamic diversity
69 (Ayala-Ortiz et al., 2023; Bahureksa et al., 2021). Recent advancements have shown the potential of
70 integrating the chemodiversity of DOM into C cycling models using bioenergetic to predict its uptake and
71 microbial growth rates (Chakrawal et al., 2022; Desmond-Le Quéméner and Bouchez, 2014; LaRowe and
72 Van Cappellen, 2011; Song et al., 2020). These approaches only account for the average thermodynamic
73 properties of DOM despite the fact that different chemical classes of DOM have varying bioavailability
74 and thermodynamic properties (Ahamed et al., 2023; Song et al., 2020). Despite a strong theoretical
75 basis, these model formulations have not been widely tested with empirical datasets. Overall, the
76 integration of high resolution FTICR-MS data into models is still new in the field of modeling soil
77 biogeochemical processes, with considerable uncertainty regarding how effectively these new data-
78 model integration approaches can capture the complexity of DOM chemodiversity and its impacts on
79 ecosystem processes.

80 Here, we adopt a two-pronged approach to (1) assess the nature of relationships between the
81 chemodiversity of DOM and soil respiration across the continental United States and (2) determine if
82 recent advances in modeling DOM chemodiversity improve continental-scale predictions of soil

83 respiration. Our overarching goal is to assess the ability of current-generation, DOM-chemistry-explicit
84 soil C models to improve predictions of soil respiration, and to identify potential interactions between
85 DOM chemodiversity and edaphic factors that may benefit from explicit representation. First, we use
86 regression analysis to evaluate various metrics of DOM chemodiversity (e.g., abundances and functional
87 diversity) to predict soil respiration in the context of common soil biogeochemical variables. We then
88 evaluate the predictive ability of three types of kinetics-based model simulations: Monod kinetics, a
89 single homogeneous DOM pool model, and a multi pool model. Monod kinetics formulates respiration as
90 a function of DOC concentration only and remains the most common method in soil carbon models. The
91 single homogeneous DOM pool model and the multi pool model are based on metabolic transition state
92 theory, which uses parameters that link soil respiration rates directly to the thermodynamic properties of
93 DOM (Desmond-Le Quéméner and Bouchez, 2014). In the homogeneous DOM pool model, we define a
94 single DOM pool by the average thermodynamic properties of the DOM. The multi pool model
95 incorporates a more detailed representation, with thermodynamic properties defined for individual
96 chemical classes of DOM. Our main hypothesis is that DOM chemodiversity is a crucial driver of soil
97 respiration; therefore, incorporating chemical diversity into kinetic parameters will improve model
98 predictions of soil respiration relative to models based on soil C concentration alone.

99 **3. Methods and Materials**

100 **3.1. Data**

101 We used standardized data collected from topsoil (0-10 cm) in 63 cores across the continental U.S.
102 (CONUS) (Figure 1A). A comprehensive set of data on soil respiration rates, water-extractable OM
103 concentration and chemistry, and over twenty additional biogeochemical parameters were collected by
104 the 1000 Soil Pilot program of the Molecular Observation Network (MONet), described by Bowman et al.
105 (2023) and Shi et al. (2024). Soil respiration rate was measured using the CO₂ burst method, and
106 dissolved SOM chemistry was assayed with Fourier-transform ion cyclotron resonance mass
107 spectrometry (FTICR-MS). Please refer to Bowman et al. (2023) for detailed methodologies regarding
108 data collection.

109 As previously described by Shi et al. (2024), FTICR-MS detected over 7,000 unique dissolved SOM
110 molecules, which were then assigned chemical formulas using CoreMS. We then used Van Krevelen
111 analysis to group molecules into nine broad molecular classes: Amino Sugar-like, Carbohydrate-like,
112 Condensed Hydrocarbon-like, Lignin-like, Lipid-like, Protein-like, Tannin-like, Unsaturated Hydrocarbon-
113 like, and Other. Van Krevelen analysis assigns an organic compound (OC) to a class if its H/C and O/C
114 ratios fall within the specified upper and lower limits for that class (Ayala-Ortiz et al., 2023; Bahureksa et
115 al., 2021; Bailey et al., 2017). Chemical classes defined only represent a class-like category because they
116 rely on elemental composition and do not capture structural complexity (e.g., lignin-like or carbohydrate-
117 like). Still, FTICR-MS provides unmatched resolution in DOM composition, enabling the detection of the
118 full range of DOM compounds using any available analytical techniques.

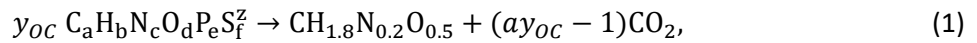
119 **3.2. Statistical analysis of soil respiration**

120 We used linear regression models to predict soil respiration as a function of biogeochemical variables
121 and DOM chemodiversity related variables calculated from FTICR-MS data (Table A1). To represent the

122 chemical nature of DOM, we used the mean nominal oxidation state of C, mean double bond equivalent,
 123 and mean molecular weight of DOM (see supplementary information for more details). Further, to
 124 quantify the chemodiversity of DOM, we used alpha diversity, indicating the number of detected organic
 125 compounds and the Shannon diversity index. In the initial model, we included soil moisture content, clay
 126 content (%), DOC and water-extractable total N concentrations, total C (%), pH, thermodynamic
 127 favorability factor (λ see eq A2), alpha diversity, and Shannon diversity index as predictors of soil
 128 respiration rates. Potential respiration was log-transformed, and all predictors were centered and scaled.
 129 We selected the best-fit linear regression following a sequential model selection approach, beginning
 130 with the most complex model (including all interaction terms) and simplifying the model based on the
 131 Akaike information criterion and log-likelihood test. We note that removing insignificant predictors can
 132 increase the Akaike information criterion; however, if the resulting model had a marginal reduction in
 133 the coefficient of determination, then we selected the simpler model regardless of the increase in the
 134 Akaike information criterion. More details on model construction are provided in the supplementary
 135 information.

136 3.3. Microbial growth reaction and growth kinetics

137 To account for the chemical diversity of DOM and its concentration while estimating soil respiration rate,
 138 we used the bioenergetic approach that allows integrating thermodynamic properties of different
 139 organic compounds as parameters in kinetic models. We used the bioenergetic framework as described
 140 in Chakrawal et al. (2022) and Song et al. (2020) to estimate the stoichiometric coefficients of the
 141 metabolic growth reaction of microorganisms under aerobic conditions and predicted microbial
 142 respiration rates from DOM chemistry (Graham et al., 2023; Zheng et al., 2024). Under aerobic
 143 conditions, the carbon balance in the metabolic growth reaction for building 1 C mole of microbial
 144 biomass ($\text{CH}_{1.8}\text{N}_{0.2}\text{O}_{0.5}$) from a general organic compound ($\text{C}_a\text{H}_b\text{N}_c\text{O}_d\text{P}_e\text{S}_f^z$) can be written as follows,



145 where y_{OC} and $y_{CO_2} = (ay_{OC} - 1)$ are the stoichiometric coefficients of organic compound and CO_2 ,
 146 respectively, calculated using the Gibbs energy balance of catabolic, anabolic, and metabolic reactions.
 147 The stoichiometric coefficient of the metabolic reaction is estimated by doing a Gibbs energy balance of
 148 catabolic (ΔG_{cat}) and anabolic parts (ΔG_{an}) of metabolic reactions (see Song et al. (2020) for details). A
 149 higher value of y_{OC} indicates a thermodynamically less favorable substrate because more substrate is
 150 utilized to produce 1C mol of biomass requiring more energy to be generated from catabolism. The
 151 carbon use efficiency of microbial growth (CUE) can be calculated as $\text{CUE} = \frac{1}{a \times y_{OC}}$.

152 We used the metabolic transition state theory (MTS) (Desmond-Le Quéméner and Bouchez, 2014) to
 153 calculate the respiration rate as a function of stoichiometric coefficients (y_{OC} and y_{CO_2}) and DOC
 154 concentration (S_{DOC}) (Table 1). For a single pool of DOM, we used average values of y_{OC} and y_{CO_2} , and
 155 the total concentration of DOC from each soil sample for estimating soil respiration rate, R_{MTS}^{mean} . In the
 156 case of multi pool model, we calculated soil respiration (R_{MTS}^{multi}) as the sum of respiration from all
 157 chemical classes of DOM considering the variation in their relative abundance and variations in model
 158 parameters y_{OC} , y_{CO_2} , and μ_{max} values for each chemical class (Table 1). Relative abundance was

159 calculated as the number of peaks within each chemical class as a percentage of total peaks. We also
 160 considered Monod kinetics with a single pool DOM as a reference model where model parameters were
 161 directly fitted using observed respiration (Table 1). Additional details on bioenergetic framework and
 162 kinetics are provided in the supplementary information.

163 In the two models based on MTS kinetics (single and multi pool), there are four model parameters: the
 164 stoichiometric coefficients y_{CO_2} and y_{OC} maximum growth rate μ_{max} , and a volume harvest
 165 parameter V_h representing accessible volume by microorganisms to acquire chemical energy from the
 166 surroundings. For each chemical class, we calculated stoichiometric coefficients directly from the growth
 167 reaction described above (eq. 1). For μ_{max} , first, we calculated the maximum substrate uptake rate
 168 (q_{max}) as a function of number of electrons (N_e) transferred from organic C to electron acceptor during
 169 catabolism following González-Cabaleiro et al. (2015). Equations for q_{max} and μ_{max} are as follows,

$$q_{max} = \frac{3}{N_e} \quad (2)$$

$$\mu_{max} = CUE q_{max} \quad (3)$$

170 Using eqs 2 and 3, in the single pool, the average μ_{max} is calculated for each soil sample, while in the
 171 multi pool model μ_{max} varies among chemical classes as well as for soil samples. We used the same
 172 approach for stoichiometric coefficients y_{CO_2} and y_{OC} in the single and multi pool models. Parameters
 173 V_h and normalization factor N in MTS, and the maximum respiration rate (V_{max}) and half saturation (K_m)
 174 in Monod kinetics were estimated as best fitted parameters by fitting the model to observed rates of soil
 175 respiration. Parameter values, model performance indices, the coefficient of determination (R^2), and root
 176 mean squared error (rmse) are provided in Table 1.

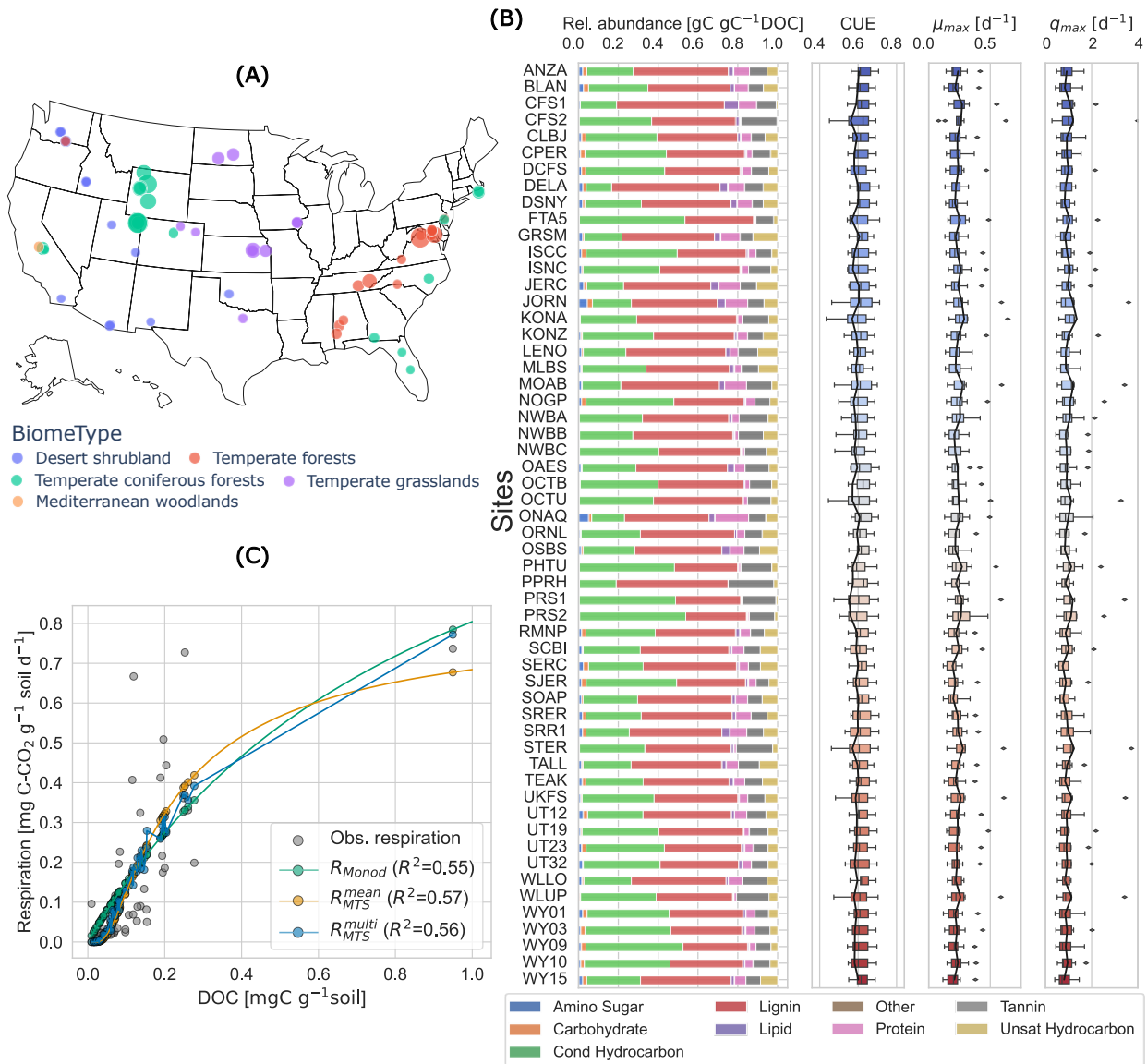
177 Table 1 Kinetic rate expression for soil respiration as a function of stoichiometric coefficients of DOM
 178 (y_{OC}) and CO_2 (y_{CO_2}), and DOC concentration (S_{DOC}) for three kinetic formulations. Estimated model
 179 parameters and model performance indices (coefficient of determination (R^2) and root mean squared
 180 error (rmse) is also included.

Model	Rate expression	Maximum rate constant (V_{max} in day^{-1}) or Normalization constant (N , in $mg\ C\ g^{-1}\ soil$)	Half saturation constant (K_M in $mg\ C\ g^{-1}\ soil$) or volume harvest parameter (V_h in $(mg\ C\ g^{-1}\ soil)^{-1}$)	R^2 [-]	rmse [$mg\ C-CO_2\ g^{-1}\ soil\ day^{-1}$]
Monod	$R_{Monod} = \frac{V_{max} S_{DOC}}{S_{DOC} + K_m}$	$V_{max} = 1.58$	$K_M = 0.935$	0.55	0.123
MTS* (Single pool)	$R_{MTS}^{mean} = N \bar{\mu}_{max} \overline{y_{CO_2}} \exp\left(-\frac{\overline{y_{OC}}}{V_h S_{DOC}}\right)$	$N = 1.8$	$V_h = 0.57$	0.57	0.120

MTS** (Multi pool)	R_{MTS}^{multi} $= N \sum_i y_{CO_2,i} \mu_{max,i} \exp\left(-\frac{y_{OCi}}{V_h S_i}\right)$	$N = 0.84$	$V_h = 1.42$	0.56	0.121
* Overline on symbol denotes average quantities.					
** S_i is the concentration of a i^{th} chemical class of DOM, and N is the normalization constant used in the data-model fitting to convert simulated respiration units to observed respiration, i.e., $mg\ C-CO_2\ g^{-1}\ soil\ day^{-1}$.					

181

182



183

184 Figure 1 (A) Location of collected soil cores with colors and size of circles illustrating biome type and soil

185 respiration rate, respectively, (B) Bar chart with relative abundance of each class of dissolved organic C

186 (in $\text{gC g}^{-1}\text{C DOC}$) and boxplots of carbon use efficiency (CUE), maximum substrate uptake rate (q_{max}) and
187 maximum growth rate (μ_{max}) across chemical classes. The solid black line denotes the mean value. (C)
188 Soil respiration as a function of DOC concentration. Observed (grey) and modeled soil respiration rates
189 using Monod kinetic R_{Monod} (green) and metabolic transition state kinetics, R_{MTS}^{mean} (single pool, yellow)
190 and R_{MTS}^{multi} (multi pool, blue).

191 **4. Results and Discussion**

192 We start by describing the observed chemodiversity of DOM in soil samples across the continental U.S.
193 (section 4.1). Next, we discuss the results from regression analysis relationships between the
194 chemodiversity of DOM and soil respiration rates (section 4.2) and compare the predicted soil
195 respiration using three kinetics models (section 4.3). We end with a broad discussion on the implications
196 and challenges of incorporating chemodiversity of DOM in biogeochemical models (section 4.4).

197 **4.1. Chemodiversity of DOM across CONUS**

198 Soil respiration rates varied spatially, with temperate forests having relatively higher rates compared to
199 other biomes (Figure 1A). Although soils displayed a high relative abundance of lignin- and condensed
200 hydrocarbon-like SOM compared to other chemical classes, there was substantial variation in the
201 proportion of these chemical classes in various soils (Figure 1). In turn, the stoichiometric coefficients
202 y_{OC} and y_{CO_2} in metabolic reaction (Figure A1) and maximum carbon use efficiency (CUE), substrate
203 uptake rate (q_{max}) and growth rate (μ_{max}) (Figure 1B) also varied across compound classes and across
204 different soils. Further, the alpha diversity of DOM varied by more than one order magnitude (range of
205 914-26933), reflecting significant chemodiversity differences in soils across CONUS (Figure A1).

206 **4.2. DOM chemodiversity interacts with biogeochemistry to explain rates of soil respiration**

207 Our goal in using the regression analysis is to build a baseline model for predicting respiration rate as a
208 function of DOM, its chemodiversity, and other biogeochemical variables. We use the regression analysis
209 to evaluate the relationship, especially, between respiration rates and DOM chemodiversity, and test
210 whether DOM chemodiversity significantly contributed to improving the prediction of respiration rates.
211 Our regression model included DOC and water-extractable total N concentrations, soil moisture, DOM
212 alpha diversity, and interactions of DOM alpha diversity with these three predictors ($R^2=0.73$, fivefold
213 cross-validation $R^2=0.62\pm 0.09$). Of these predictors, soil moisture had the highest contribution in
214 predicting soil respiration, followed by DOC concentration, DOM alpha diversity, and interaction between
215 DOC concentration and DOM alpha diversity (Table A2). Thus, supporting our hypothesis that the
216 chemical diversity of DOM can improve predictions of soil respiration, DOM and its chemical traits were
217 some of the most important statistical predictors of soil respiration rates across the continental U.S.
218 While soil moisture and DOC concentration are known drivers of soil respiration, chemodiversity is not
219 widely recognized to be an important control over organic matter decomposition rates.

220 In the following text, we discuss soil respiration as a function of DOC and water-extractable total N
221 concentrations and DOM alpha diversity. Overall, the relationship between respiration and DOM alpha
222 diversity varied with DOC and water-extractable total N concentrations (Figure 2). To explain these
223 patterns, first, we defined low resource conditions as soils with low water-extractable C concentrations

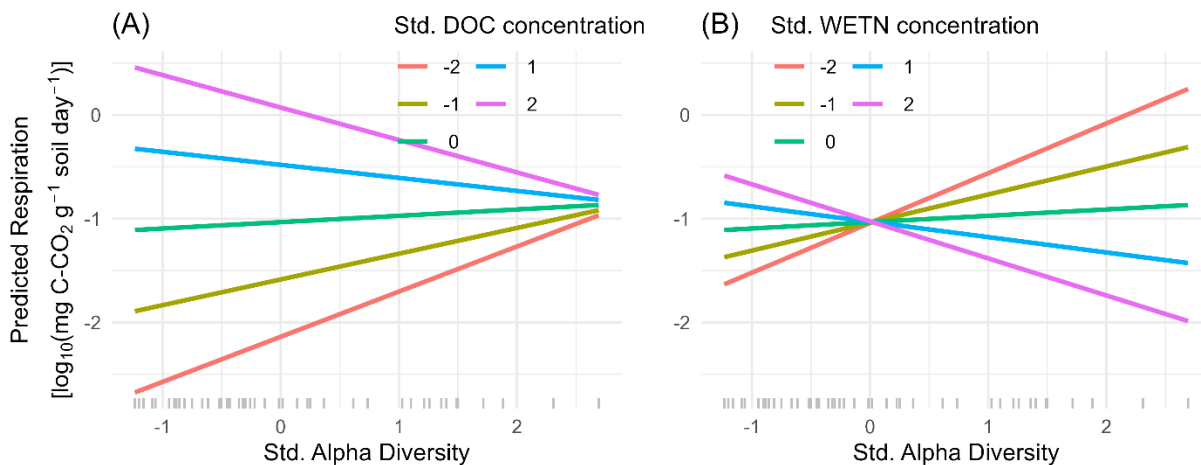
224 (DOC < avg. DOC) vs. with low water-extractable N concentrations (WETN < avg. WETN). High resource
225 conditions are assigned to soils corresponding to opposite values of C (DOC > avg. DOC) and C:N
226 (WETN > avg. WETN).

227 Under high resource conditions, DOM alpha diversity was negatively correlated with soil respiration
228 (Figure 2A for DOC > 0, and Figure 2B for WETN > 0). Higher alpha diversity also corresponded to a greater
229 proportion of putative labile compounds and high carbon use efficiency, thus favoring anabolic pathways
230 and low CO₂ production (Figure A3A-B). We can use the Yield-Acquisition-Stress (YAS) trait-based
231 paradigm of microbial metabolic strategies to explain some of these results. This paradigm defines
232 microbial communities based on their functional traits—communities adapted to maximize resources
233 towards biosynthesis with high CUE referred to as Y-strategists, communities adapted to maximize
234 resources acquisition with uptake rate referred to as A-strategists, and communities adapted to divert
235 resources into acquisition with uptake rate referred to as A-strategists (Malik et al., 2020). Here, the
236 decrease in soil respiration with increasing DOM alpha diversity under high resource conditions may
237 indicate the dominance of a Y-strategist microbial community that metabolizes bioavailable C and N for
238 growth purposes. Increased growth of microbial biomass via increased CUE has been associated with the
239 buildup of SOM through increased necromass production pathway (Tao et al., 2023); thus,
240 chemodiversity of DOM can be a critical driver of soil C persistence.

241 In contrast, under low resource conditions, DOM alpha diversity was positively correlated to soil
242 respiration (Figure 2A for DOC < 0, and Figure 2B for WETN < 0). The YAS trait-based paradigm offers a
243 plausible explanation for this relationship. Under resource limitation, microbial communities are likely to
244 invest more in the production of extracellular depolymerization enzymes that increase the bioavailability
245 of C and N (i.e., the A strategy) (Malik et al., 2020). Higher DOM alpha diversity under low resource
246 conditions may therefore trigger expression of a diverse set of enzymes, enabling the microbial
247 community to access a broader array of substrates. Consequently, under low concentrations of DOC
248 conditions with high alpha diversity of DOM, a microbial community adapted for resource acquisition
249 may dominate, and the increase in enzymatic activity in such communities can lead to elevated
250 respiration through catabolic processes that are uncoupled from biosynthetic pathways. Alternatively,
251 high DOM alpha diversity may arise from the depolymerization processes, in which chemically complex
252 DOM is decomposed into different monomers of DOM. This results in a high diversity of molecules as a
253 product of decomposition. In either case, increasing DOM alpha diversity at low DOC concentrations may
254 open new niche spaces for complementary organisms to bolster rates of metabolism (D'Andrilli et al.,
255 2019; Logue et al., 2016; Wang et al., 2022). High enzymatic activities under low resource conditions
256 indicate an increased loss of C from soils, thus suggesting that the chemodiversity of DOM may indirectly
257 control soil C loss via increased respiration.

258 The regression analysis reveals a significant nonlinear relationship between chemodiversity and soil
259 respiration, even though it does not provide mechanistic insights into how chemodiversity affects soil
260 respiration. This finding suggests that kinetic models predicting respiration rates need to account for the
261 dependency of these rates on chemodiversity. The results further indicate that DOM chemodiversity
262 could be a key factor influencing shifts in microbial metabolism and, consequently, in determining overall

263 soil respiration rates. These findings provide a basis for generating hypotheses in future studies about
 264 how DOM chemodiversity may affect microbial community responses, such as increased investment in
 265 enzymes, biosynthesis, or respiration. For instance, testing how varying degrees of DOM chemodiversity
 266 by introducing different types of labile organic compounds, while maintaining a constant DOC
 267 concentration, influences microbial metabolic tradeoffs. We anticipate that such empirical investigations
 268 will be crucial for establishing a mechanistic link between DOM chemodiversity to functional traits in
 269 microbial explicit models.



270
 271 Figure 2 Interaction plot showing the variation of soil respiration with alpha diversity for varying degrees
 272 of dissolved organic C, DOC (A), and water-extractable total N (WETN) concentrations (B) from the linear
 273 regression model. The respiration rate is in the log₁₀ transformed scale, and DOC concentration, CN
 274 ratio, and alpha diversity are on a standardized scale with a mean of zero and a standard deviation of
 275 one.

276 4.3. Comparison of kinetic models

277 In the previous section, we used empirical evidence to conclude that chemodiversity of DOM exhibits
 278 contrasting relationships to soil respiration under resource excess versus depleted conditions. This
 279 finding implies that kinetic models informed by chemodiversity should be capable of capturing this rate
 280 dependence on chemodiversity. In this section, we address this question using three kinetic models that
 281 are representative of current state-of-science modeling approaches to test whether model predictions of
 282 respiration rates improve the ability of model parameters to account for the chemodiversity of DOM.
 283 Our analysis is the first study to evaluate the calibration of kinetic models using observed soil respiration
 284 rates while also estimating model parameters using high resolution DOM chemistry at the CONUS scale.
 285 Moreover, the use of FTICR-MS data to estimate kinetics parameters can be used to reduce parameter
 286 uncertainty related to microbial processes in Earth System scale models.

287 The Monod kinetics model, which simulates respiration only as a function of DOC concentration,
 288 predicted soil respiration rates with an R^2 of approximately 0.55 (Figure 1C). When thermodynamic
 289 properties of DOM were incorporated with single pool (average μ_{max} and stoichiometric coefficients y_{OC}
 10

290 and y_{CO_2}) or with multi pool (varying μ_{max} , y_{OC} , and y_{CO_2} for discrete chemical classes), MTS kinetics
291 model predictions were similar to the Monod model ($R^2 = 0.57$ and 0.56 , respectively, Figure 1C and
292 Table 1). Overall, all kinetic models predicted rates of soil respiration less accurately than regression
293 analysis, suggesting that emerging kinetic models may still lack key processes such as tradeoffs in
294 microbial metabolic strategies (i.e., YAS traits) that may result in the observed nonlinearity in the
295 relationship between DOM alpha diversity and soil respiration.

296 Compared to other recent studies, our approach of using FTICR-MS data to predict soil respiration had
297 higher predictive power. Previous studies by Song et al. (2020) and Ahamed et al. (2023) employed a
298 similar bioenergetic approach to leverage DOM chemodiversity in predicting microbial respiration rate
299 from river systems, utilizing a fixed value of volume harvest parameter times substrate concentration,
300 i.e., $V_h S_{DOC}$ (denominator in the exponent of MTS kinetics, see Table 1). This approach does not account
301 for the variability in DOC concentration across soil samples and has resulted in a poor correlation
302 between observed and simulated respiration rates. Building on Song et al. and Ahamed et al., Zheng et
303 al. (2024), incorporated initial DOC concentration into $V_h S_{DOC}$ an MTS kinetic model using observed
304 water extracted organic C concentration while tested different values of V_h to find best correlation
305 between simulated maximum specific growth rate as a proxy for respiration with observed respiration
306 rates. Since the maximum growth rate (unit d^{-1}) and respiration rate (unit $\mu mol CO_2 g^{-1} soil d^{-1}$) are not
307 directly comparable with each other, a best fitted parameter estimation of V_h was not performed in their
308 stud, which may be the reason for low correlation and R^2 (Pearson $r = 0.56$, $R^2 = 0.19$) between modeled
309 maximum microbial growth rates and measured soil respiration rates.

310 Conversely, in our analysis, we used directly modeled CO_2 production, not maximum microbial growth
311 rate, and compared modeled predictions to measured CO_2 production. The conservation of units
312 between predicted and observed respiration allows for a more accurate comparison of model
313 performance. Furthermore, in our study, y_{OC} and y_{CO_2} in metabolic reaction (eq 1, and Figure A1), and
314 maximum carbon use efficiency (CUE), substrate uptake rate (q_{max} , eq 2 and Figure 1B) and growth rate
315 (μ_{max} , eq 3 and Figure 1B) varied across compound classes and different soils; thus, improved
316 refinement of DOM pool representation should lead to enhanced model predictions. However, we did
317 not find significant improvement across models.

318 Results from all three kinetic modeling approaches notably contrast with statistical regressions that
319 suggest that the chemodiversity of DOM is a controlling factor for shifts in microbial metabolism and,
320 thus, overall soil respiration rates. The lack of improvement in model prediction from MTS parameters
321 might be influenced by the domination of lignin- and condensed hydrocarbon-like DOM across all soil
322 samples. Consequently, MTS-predicted respiration rates are based mainly on parameters derived from
323 the same two chemical classes of DOM regardless of soil sample. Furthermore, all three kinetic models
324 deviated significantly from the 1:1 line (Figure A2), likely due to variability in soil properties, climate,
325 microbial communities, and other factors that were not included in the model.

326 Overall, regression analysis supported our hypothesis that incorporating the chemical diversity of DOM
327 improved predictions of soil respiration; however, results from kinetic models did not. This disparity

328 indicates that kinetic models for incorporating advanced DOM analytics still fail to capture process-based
329 relationships between DOM chemodiversity and soil respiration. In the next section, we explore the
330 implications of these results on the development and improvement of biogeochemical models.

331 **4.4. Implication and challenges for incorporating chemodiversity of DOM in biogeochemical models**

332 Factors driving the chemodiversity of DOM and its effects on microbial decomposition processes are
333 closely intertwined. Microbial activities contribute to the chemodiversity of DOM, while, in turn, the
334 chemodiversity of DOM influences microbial metabolism (Davenport et al., 2023; Lehmann and Kleber,
335 2015). The niche separation of microorganisms by variation in substrates, mineralogy, moisture, and
336 other environmental factors, along with the DOM chemodiversity resulting from microbial
337 decomposition (D'Andrilli et al., 2019; Logue et al., 2016; Wang et al., 2022), plays a crucial role in soil
338 respiration (Kothawala et al., 2021). This constitutes a major challenge for soil C models, specifically in
339 identifying the level of detail required to represent DOM chemodiversity while maintaining model
340 simplicity.

341 The representation of DOM chemodiversity in process-based models is usually based on a spectrum of
342 kinetic parameters used to represent slow or fast decomposition of organic matter or slow or fast
343 growing microbes (Camino-Serrano et al., 2018; Khurana et al., 2023; Wieder et al., 2015; Yu et al.,
344 2020). These approaches use kinetics parameters as a proxy for either chemical recalcitrance or shift in
345 microbial community and do not estimate model parameters as a function of the chemical properties of
346 organic matter. Newer studies are increasingly using the nominal oxidation state of organic matter to
347 characterize the decomposition and persistence of organic matter (Boye et al., 2017; Garayburu-Caruso
348 et al., 2020; Lin et al., 2021; Naughton et al., 2021). Recent efforts to include chemodiversity in soil C
349 cycle models have diverging conclusions on its control of the decomposition of DOM. For example, in
350 their theoretical model, Weverka (2023) found that microbes may invest in a diverse set of enzymes to
351 assimilate heterogenous DOM pools, or ignore some substrates in favor of others that are more
352 favorable. Both strategies result in reduced overall C assimilation rates, leading to lower DOM
353 decomposition and microbial respiration. While Khurana et al. (2023) found a positive correlation
354 between DOM chemodiversity and its decomposition rate when the chemodiversity was represented
355 using the number of organic compounds, but not when the chemodiversity was represented using
356 variation in the nominal oxidation state of C in organic compounds. These two examples highlight the
357 need for improved representation of chemodiversity of DOM in models to capture the nonlinear effects
358 of chemodiversity with soil respiration.

359 Another challenge in incorporating the effect of chemodiversity of organic matter in models is the
360 tradeoff on microbial traits with varying DOM chemodiversity. For instance, our results hint towards
361 potential tradeoffs in microbial metabolism at the community level from maximizing yield under
362 resource excess conditions vs. maximizing enzyme production under resource depleted conditions. A
363 possible solution for incorporating tradeoffs in models might be using dynamic optimization that
364 estimates optimal changes in functional traits based on the chemical composition of organic matter
365 (Chakrawal et al., 2024) or using the dynamic energy budget model that is able to resolve the tradeoff
366 between microbial growth rate and carbon use efficiency. These challenges highlight the need for further

367 investigation of novel approaches for including DOM chemodiversity in soil C cycling decomposition
368 models and developing models that are compatible with integrating the chemical diversity of soil organic
369 matter.

370 New studies have suggested the use of a more refined representation of DOM pools in mechanistic
371 models (Muller et al., 2024). However, incorporating detailed information on DOM chemistry into soil C
372 cycling models also prompts the question of whether integrating more complex representations
373 enhances model performance, especially when considering multifaceted interactions of DOM with
374 factors like soil mineralogy and microbiology (Graham and Hofmockel, 2022). In a recent work by Muller
375 et al. (2024), authors implemented multi pool representation of DOM chemodiversity in a reactive
376 transport model (Lambda-PFLOTTRAN) that can be coupled with other biological and hydrological
377 processes at the watershed scale. Such coupling between C cycling and watershed scale models that are
378 able to integrate interactions with other biogeochemical processes is a promising avenue for improving
379 the next generation of soil C cycling models, particularly if they are also extended to represent variation
380 in microbial functional traits explicitly. We note that while explicit DOM chemistry in reactive transport
381 or other ecosystem-scale models is appealing, these larger-scale frameworks often introduce additional
382 parameters, which can lead to issues like equifinality and parameter unidentifiability (Marschmann et al.,
383 2019). To address this challenge, we need widespread datasets with high molecular resolution
384 measurements. Initiatives such as the Molecular Observation Network (MONet) are facilitating high-
385 throughput molecular-scale data collection, which could mitigate this challenge. Future model
386 development efforts capable of effectively integrating these comprehensive datasets hold promise for
387 advancing our understanding of molecular scale processes and determining the requisite level of detail
388 needed in large-scale Earth System Models.

389 **5. Conclusions:**

390 In this study, we examined whether incorporating dissolved organic matter (DOM) chemodiversity into
391 predictive models of soil respiration enhances model performance. Our findings indicate a statistically
392 significant relationship between DOM alpha diversity as a measure of chemodiversity, and measured soil
393 respiration rates. However, when chemodiversity informed models were parameterized to reflect DOM
394 chemodiversity, their performance was comparable to the reference model (Monod kinetics). These
395 contrasting results suggest that the impact of DOM chemistry on soil respiration is not adequately
396 captured by emerging kinetic modeling approaches. Accurately capturing the nonlinear effect of
397 chemical diversity under varying resource conditions is essential for predicting soil C persistence, as our
398 results showed that chemodiversity controlled the plausible tradeoffs in microbial metabolism leading to
399 either loss of C through respiration or SOC buildup through increased growth.

400 **6. Funding**

401 This research was performed at the Environmental Molecular Sciences Laboratory, a DOE Office of
402 Science User Facility sponsored by the Biological and Environmental Research program under Contract
403 No. DE-AC05-76RL01830.

404 **7. Data availability**

405 The data used in this analysis is available from the 1000 Soils Pilot Dataset repository
406 <https://zenodo.org/records/7706774> with additional information on
407 <https://www.emsl.pnnl.gov/news/1000-soils-digs-data-belowground-ecosystems>.

408

409 **8. References:**

- 410 Abramoff, R., Xu, X., Hartman, M., O'Brien, S., Feng, W., Davidson, E., Finzi, A., Moorhead, D., Schimel, J.,
411 Torn, M., Mayes, M.A., 2018. The Millennial model: in search of measurable pools and
412 transformations for modeling soil carbon in the new century. *Biogeochemistry* 137, 51–71.
413 <https://doi.org/10.1007/s10533-017-0409-7>
- 414 Ahamed, F., You, Y., Burgin, A., Stegen, J.C., Scheibe, T.D., Song, H.-S., 2023. Exploring the determinants of
415 organic matter bioavailability through substrate-explicit thermodynamic modeling. *Front. Water*
416 5. <https://doi.org/10.3389/frwa.2023.1169701>
- 417 Amenabar, M.J., Shock, E.L., Roden, E.E., Peters, J.W., Boyd, E.S., 2017. Microbial substrate preference
418 dictated by energy demand rather than supply. *Nat. Geosci.* 10, 577–581.
419 <https://doi.org/10.1038/NGEO2978>
- 420 Anderson, C.G., Goebel, G.M., Tfaily, M.M., Fox, P.M., Nico, P.S., Fendorf, S., Keiluweit, M., 2023.
421 Molecular Nature of Mineral-Organic Associations within Redox-Active Mountainous Floodplain
422 Sediments. *ACS Earth Space Chem.* 7, 1623–1634.
423 <https://doi.org/10.1021/acsearthspacechem.3c00037>
- 424 Ayala-Ortiz, C., Graf-Grachet, N., Freire-Zapata, V., Fudyma, J., Hildebrand, G., AminiTabrizi, R., Howard-
425 Varona, C., Corilo, Y.E., Hess, N., Duhaime, M.B., Sullivan, M.B., Tfaily, M.M., 2023. MetaboDirect:
426 an analytical pipeline for the processing of FT-ICR MS-based metabolomic data. *Microbiome* 11,
427 28. <https://doi.org/10.1186/s40168-023-01476-3>
- 428 Bahureksa, W., Tfaily, M.M., Boiteau, R.M., Young, R.B., Logan, M.N., McKenna, A.M., Borch, T., 2021. Soil
429 Organic Matter Characterization by Fourier Transform Ion Cyclotron Resonance Mass
430 Spectrometry (FTICR MS): A Critical Review of Sample Preparation, Analysis, and Data
431 Interpretation. *Environ. Sci. Technol.* 55, 9637–9656. <https://doi.org/10.1021/acs.est.1c01135>
- 432 Bailey, V.L., Smith, A.P., Tfaily, M., Fansler, S.J., Bond-Lamberty, B., 2017. Differences in soluble organic
433 carbon chemistry in pore waters sampled from different pore size domains. *Soil Biol. Biochem.*
434 107, 133–143. <https://doi.org/10.1016/j.soilbio.2016.11.025>
- 435 Bowman, M.M., Heath, A.E., Varga, T., Battu, A.K., Chu, R.K., Toyoda, J., Cheeke, T.E., Porter, S.S., Moffett,
436 K.B., LeTendre, B., Qafoku, O., Bargar, J.R., Mans, D.M., Hess, N.J., Graham, E.B., 2023. One
437 thousand soils for molecular understanding of belowground carbon cycling. *Front. Soil Sci.* 3.
- 438 Boye, K., Noël, V., Tfaily, M.M., Bone, S.E., Williams, K.H., Bargar, J.R., Fendorf, S., 2017.
439 Thermodynamically controlled preservation of organic carbon in floodplains. *Nat. Geosci.* 10,
440 415–419. <https://doi.org/10.1038/ngeo2940>
- 441 Camino-Serrano, M., Guenet, B., Luyssaert, S., Ciais, P., Bastrikov, V., Vos, B.D., Gielen, B., Gleixner, G.,
442 Jornet-Puig, A., Kaiser, K., Kothawala, D., Lauerwald, R., Peñuelas, J., Schrumpf, M., Vicca, S.,
443 Vuichard, N., Walmsley, D., Janssens, I.A., 2018. ORCHIDEE-SOM: modeling soil organic carbon
444 (SOC) and dissolved organic carbon (DOC) dynamics along vertical soil profiles in Europe. *Geosci.*
445 *Model Dev.* 11, 937–957. <https://doi.org/10.5194/gmd-11-937-2018>
- 446 Chakrawal, A., Calabrese, S., Herrmann, A.M., Manzoni, S., 2022. Interacting Bioenergetic and
447 Stoichiometric Controls on Microbial Growth. *Front. Microbiol.* 13.

448 Chakrawal, A., Lindahl, B.D., Manzoni, S., 2024. Modelling optimal ligninolytic activity during plant litter
449 decomposition. *New Phytol.* n/a. <https://doi.org/10.1111/nph.19572>

450 D'Andrilli, J., Junker, J.R., Smith, H.J., Scholl, E.A., Foreman, C.M., 2019. DOM composition alters
451 ecosystem function during microbial processing of isolated sources. *Biogeochemistry* 142, 281–
452 298. <https://doi.org/10.1007/s10533-018-00534-5>

453 Davenport, R., Bowen, B.P., Lynch, L.M., Kosina, S.M., Shabtai, I., Northen, T.R., Lehmann, J., 2023.
454 Decomposition decreases molecular diversity and ecosystem similarity of soil organic matter.
455 *Proc. Natl. Acad. Sci.* 120, e2303335120. <https://doi.org/10.1073/pnas.2303335120>

456 Desmond-Le Quéméner, E., Bouchez, T., 2014. A thermodynamic theory of microbial growth. *ISME J.* 8,
457 1747–1751. <https://doi.org/10.1038/ismej.2014.7>

458 Ding, Y., Shi, Z., Ye, Q., Liang, Y., Liu, M., Dang, Z., Wang, Y., Liu, C., 2020. Chemodiversity of Soil Dissolved
459 Organic Matter. *Environ. Sci. Technol.* 54, 6174–6184. <https://doi.org/10.1021/acs.est.0c01136>

460 Garayburu-Caruso, V.A., Stegen, J.C., Song, H.-S., Renteria, L., Wells, J., Garcia, W., Resch, C.T., Goldman,
461 A.E., Chu, R.K., Toyoda, J., Graham, E.B., 2020. Carbon Limitation Leads to Thermodynamic
462 Regulation of Aerobic Metabolism. *Environ. Sci. Technol. Lett.* 7, 517–524.
463 <https://doi.org/10.1021/acs.estlett.0c00258>

464 González-Cabaleiro, R., Ofițeru, I.D., Lema, J.M., Rodríguez, J., 2015. Microbial catabolic activities are
465 naturally selected by metabolic energy harvest rate. *ISME J.* 9, 2630–2641.
466 <https://doi.org/10.1038/ismej.2015.69>

467 Graham, E.B., Hofmockel, K.S., 2022. Ecological stoichiometry as a foundation for omics-enabled
468 biogeochemical models of soil organic matter decomposition. *Biogeochemistry* 157, 31–50.
469 <https://doi.org/10.1007/s10533-021-00851-2>

470 Graham, E.B., Song, H.-S., Grieger, S., Garayburu-Caruso, V.A., Stegen, J.C., Bladon, K.D., Myers-Pigg, A.N.,
471 2023. Potential bioavailability of representative pyrogenic organic matter compounds in
472 comparison to natural dissolved organic matter pools. *Biogeosciences* 20, 3449–3457.
473 <https://doi.org/10.5194/bg-20-3449-2023>

474 Keiluweit, M., Bougoure, J.J., Nico, P.S., Pett-Ridge, J., Weber, P.K., Kleber, M., 2015. Mineral protection of
475 soil carbon counteracted by root exudates. *Nat. Clim. Change* 5, 588–595.
476 <https://doi.org/10.1038/nclimate2580>

477 Khurana, S., Abramoff, R., Bruni, E., Dondini, M., Tupek, B., Guenet, B., Lehtonen, A., Manzoni, S., 2023.
478 Interactive effects of microbial functional diversity and carbon availability on decomposition – A
479 theoretical exploration. *Ecol. Model.* 486, 110507.
480 <https://doi.org/10.1016/j.ecolmodel.2023.110507>

481 Kothawala, D.N., Kellerman, A.M., Catalán, N., Tranvik, L.J., 2021. Organic Matter Degradation across
482 Ecosystem Boundaries: The Need for a Unified Conceptualization. *Trends Ecol. Evol.* 36, 113–122.
483 <https://doi.org/10.1016/j.tree.2020.10.006>

484 LaRowe, D.E., Van Cappellen, P., 2011. Degradation of natural organic matter: A thermodynamic analysis.
485 *Geochim. Cosmochim. Acta* 75, 2030–2042. <https://doi.org/10.1016/j.gca.2011.01.020>

486 Lehmann, J., Kleber, M., 2015. The contentious nature of soil organic matter. *Nature*.
487 <https://doi.org/10.1038/nature16069>

488 Lin, Y., Campbell, A.N., Bhattacharyya, A., DiDonato, N., Thompson, A.M., Tfaily, M.M., Nico, P.S., Silver,
489 W.L., Pett-Ridge, J., 2021. Differential effects of redox conditions on the decomposition of litter
490 and soil organic matter. *Biogeochemistry*. <https://doi.org/10.1007/s10533-021-00790-y>

491 Logue, J.B., Stedmon, C.A., Kellerman, A.M., Nielsen, N.J., Andersson, A.F., Laudon, H., Lindström, E.S.,
492 Kritzberg, E.S., 2016. Experimental insights into the importance of aquatic bacterial community
493 composition to the degradation of dissolved organic matter. *ISME J.* 10, 533–545.
494 <https://doi.org/10.1038/ismej.2015.131>

495 Lv, J., Huang, Z., Christie, P., Zhang, S., 2020. Reducing Reagents Induce Molecular Artifacts in the
 496 Extraction of Soil Organic Matter. *ACS Earth Space Chem.* 4, 1913–1919.
 497 <https://doi.org/10.1021/acsearthspacechem.0c00194>
 498 Malik, A.A., Martiny, J.B.H., Brodie, E.L., Martiny, A.C., Treseder, K.K., Allison, S.D., 2020. Defining trait-
 499 based microbial strategies with consequences for soil carbon cycling under climate change. *ISME*
 500 *J.* 14, 1–9. <https://doi.org/10.1038/s41396-019-0510-0>
 501 Marschmann, G.L., Pagel, H., Kögler, P., Streck, T., 2019. Equifinality, sloppiness, and emergent structures
 502 of mechanistic soil biogeochemical models. *Environ. Model. Softw.* 122, 104518.
 503 <https://doi.org/10.1016/j.envsoft.2019.104518>
 504 Marschmann, G.L., Tang, J., Zhalnina, K., Karaoz, U., Cho, H., Le, B., Pett-Ridge, J., Brodie, E.L., 2024.
 505 Predictions of rhizosphere microbiome dynamics with a genome-informed and trait-based
 506 energy budget model. *Nat. Microbiol.* 9, 421–433. <https://doi.org/10.1038/s41564-023-01582-w>
 507 Moyano, F.E., Manzoni, S., Chenu, C., 2013. Responses of soil heterotrophic respiration to moisture
 508 availability: An exploration of processes and models. *Soil Biol. Biochem.* 59, 72–85.
 509 <https://doi.org/10.1016/j.soilbio.2013.01.002>
 510 Muller, K.A., Jiang, P., Hammond, G., Ahmadullah, T., Song, H.-S., Kukkadapu, R., Ward, N., Bowe, M.,
 511 Chu, R.K., Zhao, Q., Garayburu-Caruso, V.A., Roebuck, A., Chen, X., 2024. Lambda-PFLOTRAN 1.0:
 512 Workflow for Incorporating Organic Matter Chemistry Informed by Ultra High Resolution Mass
 513 Spectrometry into Biogeochemical Modeling. <https://doi.org/10.5194/gmd-2024-34>
 514 Naughton, H.R., Keiluweit, M., Tfaily, M.M., Dynes, J.J., Regier, T., Fendorf, S., 2021. Development of
 515 energetic and enzymatic limitations on microbial carbon cycling in soils. *Biogeochemistry* 153,
 516 191–213. <https://doi.org/10.1007/s10533-021-00781-z>
 517 Parton, W.J., Ojima, D.S., Cole, C.V., Schimel, D.S., 1994. A General Model for Soil Organic Matter
 518 Dynamics: Sensitivity to Litter Chemistry, Texture and Management, in: *Quantitative Modeling of*
 519 *Soil Forming Processes*. John Wiley & Sons, Ltd, pp. 147–167.
 520 Robertson, A.D., Paustian, K., Ogle, S., Wallenstein, M.D., Lugato, E., Cotrufo, M.F., 2019. Unifying soil
 521 organic matter formation and persistence frameworks: the MEMS model. *Biogeosciences* 16,
 522 1225–1248. <https://doi.org/10.5194/bg-16-1225-2019>
 523 Shi, C., Mudunuru, M., Bowman, M., Zhao, Q., Toyoda, J., Kew, W., Corilo, Y., Qafoku, O., Bargar, J.R.,
 524 Karra, S., Graham, E., 2024. Scaling High-resolution Soil Organic Matter Composition to Improve
 525 Predictions of Potential Soil Respiration Across the Continental United States.
 526 Sokol, N.W., Sanderman, J., Bradford, M.A., 2019. Pathways of mineral-associated soil organic matter
 527 formation: Integrating the role of plant carbon source, chemistry, and point of entry. *Glob.*
 528 *Change Biol.* 25, 12–24. <https://doi.org/10.1111/gcb.14482>
 529 Song, H.-S., Stegen, J.C., Graham, E.B., Lee, J.-Y., Garayburu-Caruso, V.A., Nelson, W.C., Chen, X., Moulton,
 530 J.D., Scheibe, T.D., 2020. Representing Organic Matter Thermodynamics in Biogeochemical
 531 Reactions via Substrate-Explicit Modeling. *Front. Microbiol.* 11.
 532 <https://doi.org/10.3389/fmicb.2020.531756>
 533 Tanentzap, A.J., Fonvielle, J.A., 2024. Chemodiversity in freshwater health. *Science* 383, 1412–1414.
 534 <https://doi.org/10.1126/science.adg8658>
 535 Tao, F., Huang, Y., Hungate, B.A., Manzoni, S., Frey, S.D., Schmidt, M.W.I., Reichstein, M., Carvalhais, N.,
 536 Ciais, P., Jiang, L., Lehmann, J., Wang, Y.-P., Houlton, B.Z., Ahrens, B., Mishra, U., Hugelius, G.,
 537 Hocking, T.D., Lu, X., Shi, Z., Viatkin, K., Vargas, R., Yigini, Y., Omuto, C., Malik, A.A., Peralta, G.,
 538 Cuevas-Corona, R., Di Paolo, L.E., Luotto, I., Liao, C., Liang, Y.-S., Saynes, V.S., Huang, X., Luo, Y.,
 539 2023. Microbial carbon use efficiency promotes global soil carbon storage. *Nature* 618, 981–985.
 540 <https://doi.org/10.1038/s41586-023-06042-3>

541 Wang, G., Post, W.M., Mayes, M.A., 2013. Development of microbial-enzyme-mediated decomposition
542 model parameters through steady-state and dynamic analyses. *Ecol. Appl.* 23, 255–272.
543 <https://doi.org/10.1890/12-0681.1>

544 Wang, Y., Xie, R., Shen, Y., Cai, R., He, C., Chen, Q., Guo, W., Shi, Q., Jiao, N., Zheng, Q., 2022. Linking
545 Microbial Population Succession and DOM Molecular Changes in Synechococcus-Derived Organic
546 Matter Addition Incubation. *Microbiol. Spectr.* 10, e02308-21.
547 <https://doi.org/10.1128/spectrum.02308-21>

548 Weverka, J.R., Moeller, H.V., Schimel, J.P., 2023. Chemodiversity controls microbial assimilation of soil
549 organic carbon: A theoretical model. *Soil Biol. Biochem.* 187, 109161.
550 <https://doi.org/10.1016/j.soilbio.2023.109161>

551 Wieder, W.R., Grandy, A.S., Kallenbach, C.M., Bonan, G.B., 2014. Integrating microbial physiology and
552 physio-chemical principles in soils with the Microbial-MIneral Carbon Stabilization (MIMICS)
553 model. *Biogeosciences* 11, 3899–3917. <https://doi.org/10.5194/bg-11-3899-2014>

554 Wieder, W.R., Grandy, A.S., Kallenbach, C.M., Taylor, P.G., Bonan, G.B., 2015. Representing life in the
555 Earth system with soil microbial functional traits in the MIMICS model. *Geosci. Model Dev.* 8,
556 1789–1808. <https://doi.org/10.5194/gmd-8-1789-2015>

557 Witzgall, K., Vidal, A., Schubert, D.I., Höschel, C., Schweizer, S.A., Buegger, F., Pouteau, V., Chenu, C.,
558 Mueller, C.W., 2021. Particulate organic matter as a functional soil component for persistent soil
559 organic carbon. *Nat. Commun.* 12, 4115. <https://doi.org/10.1038/s41467-021-24192-8>

560 Wutzler, T., Zaehle, S., Schrumpf, M., Ahrens, B., Reichstein, M., 2017. Adaptation of microbial resource
561 allocation affects modelled long term soil organic matter and nutrient cycling. *Soil Biol. Biochem.*
562 115, 322–336. <https://doi.org/10.1016/j.soilbio.2017.08.031>

563 Yu, L., Ahrens, B., Wutzler, T., Schrumpf, M., Zaehle, S., 2020. Jena Soil Model (JSM v1.0; revision 1934): a
564 microbial soil organic carbon model integrated with nitrogen and phosphorus processes. *Geosci.*
565 *Model Dev.* 13, 783–803. <https://doi.org/10.5194/gmd-13-783-2020>

566 Zheng, J., Scheibe, T.D., Boye, K., Song, H.-S., 2024. Thermodynamic control on the decomposition of
567 organic matter across different electron acceptors. *Soil Biol. Biochem.* 193, 109364.
568 <https://doi.org/10.1016/j.soilbio.2024.109364>
569

570

571

572 **Supplementary information**

573 Challenges in Integrating DOM Chemodiversity into Kinetic Models of Soil Respiration for Improved
574 Carbon Cycling Predictions

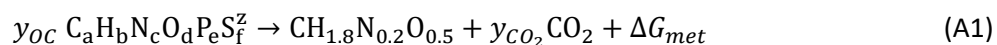
575 Arjun Chakrawal¹, Odeta Qafoku¹, Satish Karra¹, John Bargar¹, and Emily Graham^{1,2}

576 ¹Environmental Molecular Sciences Laboratory (EMSL), Pacific Northwest National Laboratory, PO Box
577 999, Richland, WA 99352, USA

578 ²School of Biological Sciences, Washington State University, Pullman, WA, USA

579 **1. Microbial growth reaction and growth kinetics**

580 Under aerobic conditions, the carbon balance of a metabolic growth reaction for building 1 C mole of
581 microbial biomass from a general bioavailable dissolved organic compound (DOC, C_aH_bN_cO_dP_eS_f^Z) can
582 be written as follows,



583 where C_aH_bN_cO_dP_eS_f^Z represents a generic OC, CH_{1.8}N_{0.2}O_{0.5} is a chemical representation of microbial
584 biomass, and y_{OC} and y_{CO_2} are the stoichiometric coefficients of DOC and CO₂. The stoichiometric
585 coefficient of the metabolic reaction is estimated by doing a change in Gibbs energy balance of catabolic
586 (ΔG_{cat}) and anabolic parts (ΔG_{an}) of metabolic reactions. The ratio of the sum of Gibbs energy
587 dissipated and conserved in biomass to Gibbs generated from catabolism is defined as the
588 thermodynamic favorability factor λ as follows,

$$\lambda_i = \frac{\Delta G_{diss_i} + \Delta G_{an_i}}{-\Delta G_{cat_i}} \quad (A2)$$

589 The subscript i represent the class of organic carbon. For details in calculating the change in Gibbs
590 energy values for catabolic and anabolic reaction reader are referred to (Kleerebezem and Van
591 Loosdrecht, 2010; LaRowe and Van Cappellen, 2011; Song et al., 2020; Chakrawal et al., 2022). The
592 change in Gibbs energy was also corrected for observed pH in soil pore water (Amend and LaRowe,
593 2019; Song et al., 2020).

594 A higher value of λ_i denotes less favorable substrate because catabolism needs to run a greater number
595 of times to produce 1C mol of biomass, requiring more energy to be generated from catabolism. The
596 stoichiometric coefficients of DOC and CO₂ can be calculated as a function of λ as follows,

$$y_{OC_i} = \lambda_i + y_{OC_i}^{an} \quad (A3)$$

$$y_{CO_2_i} = y_{OC_i} a - 1, \quad (A4)$$

597 where $y_{OC_i}^{an}$ is the stoichiometric coefficient of DOC in the anabolic reaction, and a is the number of C
598 atoms in the chemical formula of DOC. Note that the change in Gibbs energy values was corrected for
599 measured soil pH (Kleerebezem and Van Loosdrecht, 2010).

600 Next, we used the metabolic transition state theory (Desmond-Le Quéméner and Bouchez, 2014) to
 601 calculate the respiration rate (R_{CO_2i}),

$$R_{CO_2i} = N y_{CO_2i} \mu_i^{max} \exp\left(-\frac{y_{OCi}}{V_h S_{DOC,i}}\right), \quad (A5)$$

602 where μ_i^{max} is the maximum growth rate (d^{-1}) and $S_{DOC,i}$ is the concentration of DOC (mg C g^{-1} soil) of
 603 each class of organic compound, and V_h is a kinetic parameter representing accessible volume by
 604 microorganisms to acquire chemical energy from the surroundings ((mg C g^{-1} soil) $^{-1}$) and N is a
 605 normalization factor (mg C g^{-1} soil). The concentration of each class of compound was calculated as their
 606 relative abundance multiplied by the total concentration of DOC for the given soil sample.

607 For a single pool DOM kinetic model, DOM is considered to be chemically homogeneous, and kinetic
 608 parameters are estimated using the average thermodynamic properties of the DOM. The respiration for
 609 a single pool model can be written as follows,

$$R_{MST}^{mean} = N \bar{\mu}_{max} \bar{y}_{CO_2} \exp\left(-\frac{\bar{y}_{OC}}{V_h S_{DOC}}\right) \quad (A6)$$

610 The overline symbols represent average statistics across nine classes of OCs. The respiration for a multi-
 611 pool model is calculated as the sum of respiration from all classes considering the variation in their
 612 relative abundance and thermodynamic favorability, and can be written as follows,

$$R_{MST}^{multi} = N \sum_i y_{CO_2,i} \mu_{max,i} \exp\left(-\frac{y_{OCi}}{V_h S_i}\right) \quad (A7)$$

613 Modelled respiration in both MTS based models have the units of mg C g^{-1} soil day^{-1} . As a reference
 614 model that does not include aspects of the chemodiversity of DOM, we used Monod kinetics to predict
 615 respiration as a function of DOC concentration. The respiration rate using Monod kinetics can be written
 616 as,

$$R_{Monod} = \frac{V_{max} S_{DOC}}{S_{DOC} + K_m} \quad (A8)$$

617 where V_{max} and K_M are maximum respiration rate (mg C g^{-1} soil day^{-1}) and half saturation constant (mg C
 618 g^{-1} soil), respectively.

619

620 2. Statistical analyses

621 We used linear mixed effect models for predicting soil respiration as a function of other biogeochemical
 622 variables, and DOM chemodiversity related variables were calculated from FTICR-MS data. To represent
 623 the chemical nature of DOM, we used the mean thermodynamic favorability factor, lambda (eq A2,
 624 (Song et al., 2020)), mean double bond equivalent (DBE), and mean molecular weight of DOC
 625 (calculation provided in following section). Further, to represent chemodiversity of DOM, we used alpha

626 diversity indicating the number of detected organic compounds, coefficient of variation in lambda, and
627 Shannon diversity index. For robust model selection, first, we removed predictors with insignificant
628 correlation with respiration using p-value>0.05 threshold in Pearson correlation coefficient, and then, we
629 removed multicollinear predictors with correlation coefficients of more than 0.7.

630 For a preliminary model, we included soil moisture content, clay content (%), DOC and water-extractable
631 total N (WETN) concentrations, total C (%), pH, thermodynamic favorability factor (λ see eq A2), alpha
632 diversity and Shannon diversity index as predictors. To enhance interpretability, respiration was log10-
633 transformed, and all predictors were centered and scaled. In the linear mixed effect model, biome type
634 was used as a random effect on intercept; however, later, it was dropped due to the high Akaike
635 information criterion compared to the linear model as a base model. We selected the best-fit linear
636 regression following a sequential model selection approach, beginning with the most complex model
637 (including all interaction terms) and simplifying the model based on the Akaike information criterion and
638 log-likelihood test. We note that removing insignificant predictors can increase AIC; however, if the
639 resulting model had a marginal reduction in coefficient of determination, then we selected the simpler
640 model regardless of the increase in AIC.

641 Regression analysis was performed using R statistical software (R Core Team, 2023), version 4.3.2. The
642 analysis utilized the nlme package (Pinheiro et al., 2023) for mixed-effects models. For estimating
643 individual contribution of predictors in predicting respiration rate, we used lmg function from relaimpo
644 package (Groemping, 2007) that decompose overall R-squared for fit to R-squared explained by
645 individual predictors while accounting for the correlation structure among predictors and predictors
646 ordering in the regression formula. Lastly, for summarizing regression results in tabular format, the
647 modelsummary package (Arel-Bundock, 2022) was employed.

648 **2.1. Nominal oxidation state of carbon and double bond equivalent**

649 The nominal oxidation state of carbon (NOSC) in an organic compound ($C_aH_bN_cO_dP_eS_f^z$) is defined as
650 following,

$$651 \quad NOSC = 4 - \frac{4a + b - 3c - 2d + 5e - 2f - n_z}{a} \quad (A9)$$

651 The NOSC ranges from -4 for most reduced state of C in CH_4 and +4 for most oxidized state of C in CO_2
652 (LaRowe and Van Cappellen, 2011).

653 The double bond equivalent (DBE) is used to estimate the degree of unsaturation (i.e., the presence of
654 double, triple bond or rings in chemical structure) in an organic compound (Koch and Dittmar, 2006) and
655 calculated as follows,

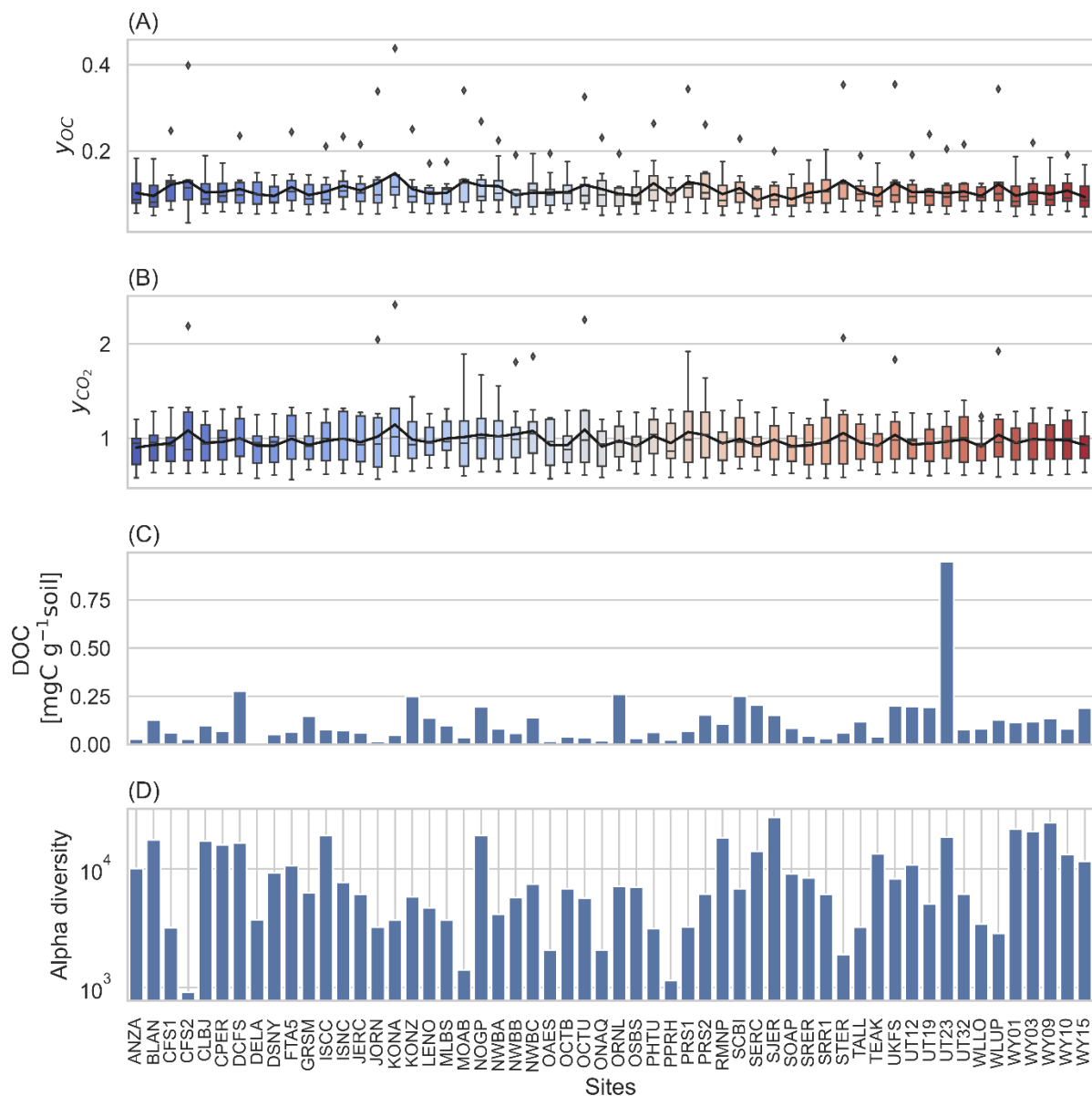
$$656 \quad DBE = 1 + 0.5 (2a - b + c) \quad (A10)$$

656 **2.2. Shannon diversity index**

657 Shannon diversity index (Sh) provides a measure of entropy of the population, here, the population is
658 chemically diverse DOM, and calculated as,

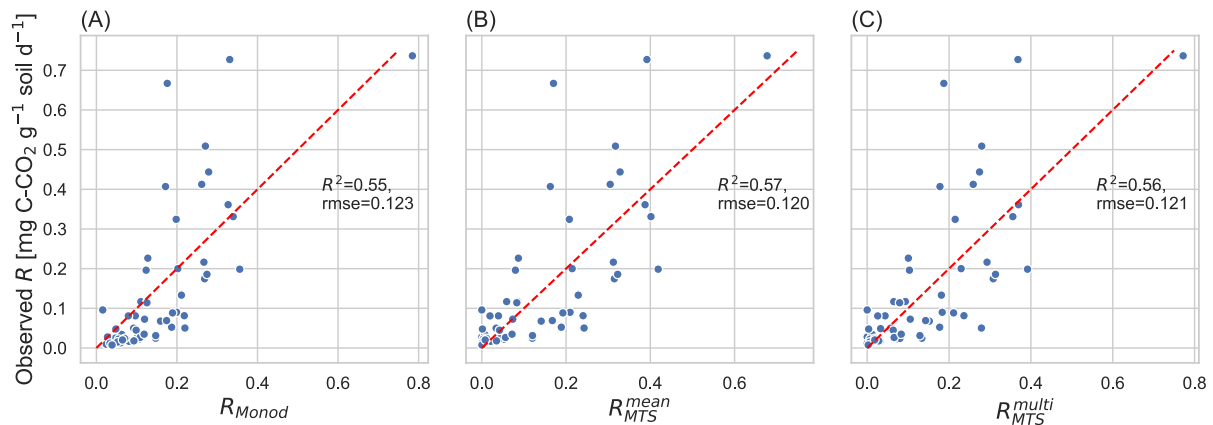
$$Sh = \sum_{i=1}^n p_i \ln p_i \quad (\text{A11})$$

659 where $n=9$ is the total number of chemical classes, and p_i is the relative abundance of each chemical
660 class.



661
 662 Figure A1 Stoichiometry of organic compound y_{OC} (A) and CO_2 y_{CO_2} (B) in the metabolic growth reaction,
 663 DOC concentration (C), and alpha diversity, i.e., species richness of DOM for each soil sample (D). The
 664 box plots of y_{OC} and y_{CO_2} show the variation across different chemical classes, and the solid black line is
 665 the mean value.

666

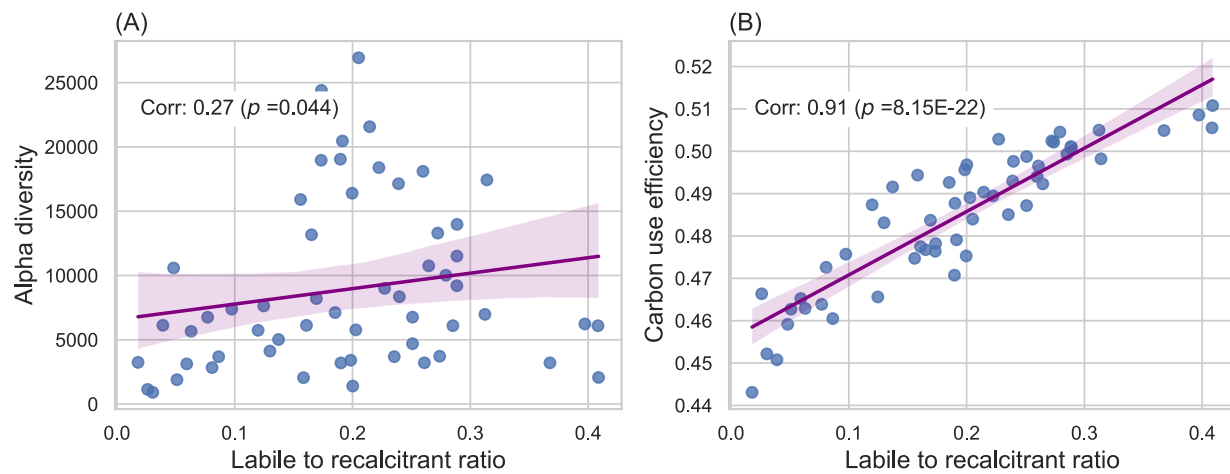


667

668 Figure A2 Scatterplot of observed and simulated respiration rates using Monod kinetics (A), using
 669 metabolic transition state kinetics with single pool DOM (B), and multiple pool DOM (C). The annotation
 670 text, R^2 and rmse are the coefficient of determination and root mean square error, respectively.

671

672



673

674 Figure A3 Alpha diversity of DOM (A) and carbon use efficiency (B) as a function of the ratio of labile to
 675 recalcitrant organic compounds. Carbohydrates, proteins, amino sugars, lipids, unsaturated
 676 hydrocarbons, and other compounds were taken as labile pools, whereas lignins, condensed
 677 hydrocarbons, and tannins were considered as recalcitrant compounds. The annotated text, *Corr* and *p*,
 678 denote the Spearman correlation and corresponding p-value, respectively.

679

680

681

682

683

684 Table A1 Coefficient estimates and model fit statistics from linear regression for predicting respiration
685 across different models during model selection process

	Alternate Model	<i>Final model</i>
(Intercept)	-0.98 (0.05)***	-1.03 (0.05)***
DOC	0.39 (0.08)***	0.55 (0.10)***
Total C (%)	0.24 (0.07)***	
WETN		0.00 (0.07)
alpha diversity	0.04 (0.05)	0.06 (0.05)
DOC × Total C (%)		
DOC × alpha diversity	-0.20 (0.06)**	-0.19 (0.09)*
WETN × pH		
WETN × alpha diversity		-0.21 (0.10)*
soil moisture	0.07 (0.06)	0.13 (0.05)*
Total C (%) × soil moisture	-0.11 (0.05)*	
soil moisture × alpha diversity		0.13 (0.05)*
Num.Obs.	52	52
R2	0.750	0.733
AIC	26.7	32.3
<p>DOC: dissolved organic C concentration, SD: standard deviation, Num.Obs.: number of observations, R² coefficient of determination in linear regression. Values within parentheses represent the standard error of the estimate. Significance levels: *** p < 0.001, ** p < 0.01, * p < 0.05, . p < 0.1, + p > 0.1</p>		

686

687 Table A2 R-square decomposition among predictors of final model in Table A1

Predictor	R²
soil moisture	0.20
DOC	0.18
alpha diversity	0.11
DOC × alpha diversity	0.09
WETN × alpha diversity	0.07
WETN	0.06

soil moisture × alpha diversity	0.02
sum of R^2	0.73

688

689

690